ACS OMEGA

http://pubs.acs.org/journal/acsodf

Article

Experimental and Kinetic Modeling Study on High-Temperature Autoignition of Cyclohexene

Jinhu Liang,* Fei Li, Shutong Cao, Xiaoliang Li, Ruining He, Ming-Xu Jia, and Quan-De Wang*

Cite This: *ACS Omega* 2022, 7, 28118−28128

Read Online

ACCESS | Metrics & More | Article Recommendations | Supporting Information

ABSTRACT: Cyclohexene is an important intermediate during the oxidation of cycloalkanes, which comprise a significant portion of real fuels. Thus, experimental data sets and kinetic models of cyclohexene play an important role in the understanding of the combustion of cycloalkanes and real fuels. In this work, an experimental and kinetic modeling study of the high-temperature ignition of cyclohexene is performed. Ignition delay time (IDT) measurements are carried out in a high-pressure shock tube (HPST). The studied pressures are 5, 10, and 20 bar; the equivalence ratios are 0.5, 1.0, and 2.0; and the temperatures range from 980 to 1400 K for IDT in HPST. It is shown that the IDTs of cyclohexene exhibit Arrhenius behaviors as a function of temperature, and the IDTs decrease as the equivalence ratio and pressure increase. The experimental results are simulated using three previous detailed kinetic mechanisms and an updated detailed mechanism in this work. The updated detailed kinetic mechanism exhibits good agreement with experimental results. Reaction path analysis and sensitivity analysis are performed to provide insights into the chemical kinetics controlling the ignition of cyclohexene. The results demonstrate that different detailed kinetic mechanisms are significantly different, and there are still no unified conclusions about the major reaction path for cyclohexene oxidation. However, it is worth noting that the abstraction reaction by oxygen at the allylic site and the submechanism of cyclopentene are of significant importance for the accurate prediction of IDTs of cyclohexene. The present experimental data set and kinetic model should be valuable to improve our understanding of the combustion chemistry of cycloalkanes.

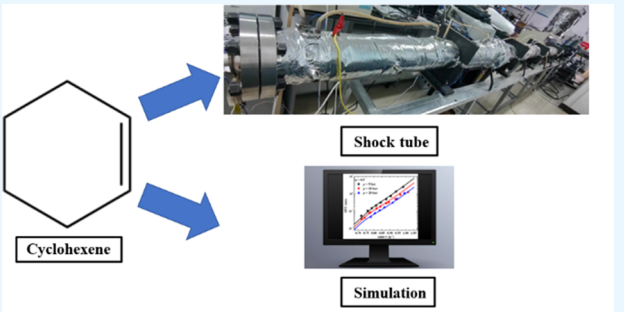

1. INTRODUCTION

Cycloalkanes represent an important class of ingredients in real fuels, i.e., gasoline, diesel, and jet fuels.[1−3] Thus, a better understanding of the combustion characteristics and combustion chemical kinetics of real fuels requires a fundamental understanding of the combustion chemistry of cycloalkanes.[4,5] During the past decades, various experimental measurements have been performed to obtain the combustion properties of cycloalkanes, i.e., ignition, flame speed, soot tendency, and species profiles during the oxidation of cycloalkanes with various molecular structures.[6−13] Detailed kinetic models are also developed to simulate experimental measurements and to gain insight into the fundamental chemical kinetics during fuel combustion.[7,10,12,14−16]

Previous studies have shown that unsaturated cyclic hydrocarbons can be rapidly obtained during the oxidation of cycloalkanes, and they play an important role in the oxidation of cycloalkanes.[10,17,18] However, very fewer work has been performed to systematically investigate the oxidation and pyrolysis process of unsaturated cyclic hydrocarbons. Cyclohexene, the simplest C_6 unsaturated cyclic hydrocarbons, has been detected in a large amount during the oxidation of methylcyclohexane and ethylcyclohexane.[10,17] Previous sensitivity analysis and reaction path analysis results indicated that the cyclohexene submechanism is important in accurately predicting the combustion properties of cycloalkanes.[10,17] Thus, the development of a kinetic mechanism for cyclohexene together with experimental studies to derive mechanism validation targets, i.e., ignition and laminar flame speed, is of crucial importance in mechanism development for cycloalkanes. But experimental and kinetic modeling studies on cyclohexene are very scarce. A systematic study on the ignition property of cyclohexene was reported by Dayma et al.,[19] who used a shock tube facility and kinetic modeling to provide a better understanding of its ignition characteristics. Other studies on cyclohexene and related unsaturated cyclic hydrocarbons are usually for specific purposes, i.e., soot formation. Kim et al. studied the soot tendencies of cyclohexene and methyl cyclohexene isomers using experimental and theoretical calculations,[13] while Wang et al. studied the benzene formation

Received: April 10, 2022
Accepted: July 28, 2022
Published: August 5, 2022

pathway during the pyrolysis of cyclohexene.[20] Giarracca et al. performed experimental and kinetic modeling studies on the ignition of cyclohexane, cyclohexene, and cyclohexadiene to demonstrate the unsaturation effect.[21] However, large discrepancies exist between the experimentally measured ignition delay time (IDT) and modeling results. Further, after a detailed survey of existing detailed mechanisms related to cyclohexene,[16,20] some of them assumed that the initial reactions of cyclohexene were thermal decomposition to ethylene and 1,3-butadiene and the abstraction reactions at the allylic site by neglecting the other reaction sites, which is too simplified.

Based on the above considerations, this work first performs an ignition study of cyclohexene under high-temperature conditions using a high-pressure shock tube (HPST). The measured experimental results are simulated using three detailed chemical kinetic mechanisms. An updated detailed mechanism based on the NUIGMech1.1 core mechanism[22] has been developed, which shows better performance in the prediction of IDTs. Reaction path analysis and sensitivity analysis are then performed to provide insight into the kinetics controlling the ignition of cyclohexene.

2. EXPERIMENTAL METHODS

The IDT experiments were performed in a high-pressure shock tube at the North University of China (NUC). The facility has been detailed in previous studies,[3,23] and thus is briefly described here. The HPST is composed of a 3.0 m driver section, a 6.8 m driven section, and a 0.3 m double diaphragm section connecting the driven and driver sections with an inner diameter of 100 mm. The incident shock velocity is measured using five PCB 113B26 piezoelectric pressure transducers mounted on the sidewall of the driven section. The pressure transducer mounted 20 mm from the end wall of the driven section was used to record the pressure-time profiles. All pressure and emission signals are recorded using two digital TiePie Handyscope HS4 oscilloscopes. The reflected wave pressure and temperature are determined using the one-dimensional normal shock relations by the Gaseq program.[24] The pressures and emissions of OH* at 306.5 nm behind reflected shock waves are recorded after bursting of the diaphragms. IDT is defined as the time interval between the arrival of the reflected shock wave and the onset of OH* emission at the side wall observation location. From Figure 1, it can be seen that the maximum rate of increase of the pressure signal is consistent with the sudden increase in the OH signal. The onset of ignition is observed in the OH* emission history defined by linearly extrapolating the maximum slope to the baseline of the emission trace. Figure 1 shows an example of the pressure and OH* emission signal traces for cyclohexene in air. It can be seen that the IDTs measured by the onset of OH* emission and the maximum rate of increase of the pressure signal are almost the same.

All mixtures are prepared in stainless-steel mixture tanks according to Dalton's law of partial pressure, and the prepared mixture is maintained at least 12 h before experiments to ensure complete vaporization and homogeneity. A glass syringe is used to extract a certain amount of liquid fuel and then fill it into the stainless-steel mixture tanks through the injection port of the gas distribution pipeline. The purities of oxygen and nitrogen used in this experiment are larger than 99.5%. Helium is used as driven gas in HPST, and the purity is also 99.99%. Cyclohexene was provided by Shanghai Macklin Biochemical

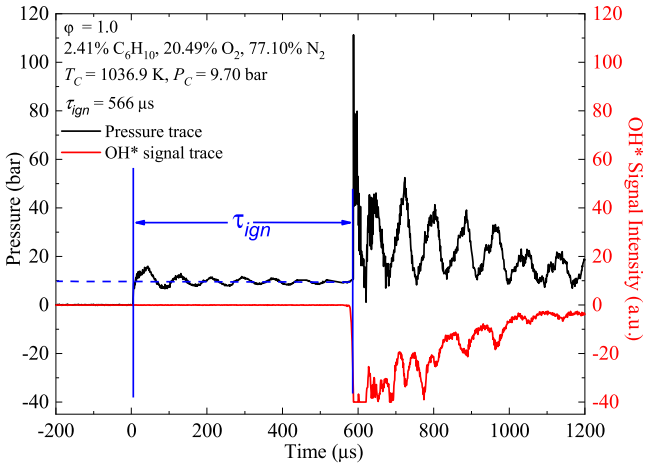

Figure 1. Typical pressure and OH* emission signal traces for cyclohexene measured in this work. The equivalence ratio is 1.0 (compositions are shown in Table 1) with initial temperature and pressure at 1036.9 K and 9.7 bar, respectively. The left and right *y*-axis denote the pressure signal and the OH* emission signal at the same experimental condition, respectively.

Co., Ltd. with a 99.0% purity. A heating system with seven thermocouples placed along the mixing tank, shock tube, and the sampling tube was used to maintain the experimental system with a temperature of 398 K to avoid adsorption of the liquid fuel. Table 1 lists the HPST experimental conditions in this work. The overall uncertainty in the measured IDTs from HPST can be controlled within ±20% based on previous analysis,[3,23] and are generally consistent with the other related facilities.[25−28]

Table 1. Experimental Conditions in this Work

equivalence ratio (φ)	reactant mixture (mol %)			avg. P_5(bar)	T_5 range (K)
	cyclohexene	O_2	N_2		
0.5	1.22	20.74	78.04	5.02	1060−1400
0.5	1.22	20.74	78.04	9.90	980−1400
0.5	1.22	20.74	78.04	19.97	1000−1300
1.0	2.41	20.49	77.10	4.95	1000−1380
1.0	2.41	20.49	77.10	9.92	1000−1320
1.0	2.41	20.49	77.10	19.86	945−1200
2.0	4.71	20.01	75.28	5.03	1000−1400
2.0	4.71	20.01	75.28	9.95	1000−1400
2.0	4.71	20.01	75.28	20.18	950−1180

3. CHEMICAL KINETIC MODELING

In this work, three previously developed detailed mechanisms, i.e., the JetSurF 2.0 mechanism[16] and the mechanisms developed by Serinyel et al.[29] and Giarracca et al.[21] are first used to simulate the measured IDTs. Specifically, the JetSurF 2.0 mechanism was developed for high-temperature combustion chemistry of mono-cyclohexanes from cyclohexane to *n*-butyl cyclohexane, and the chemical kinetics of cyclohexene was simplified. The Serinyel mechanism[29] was developed to predict the measured species profiles of low- and high-

https://doi.org/10.1021/acsomega.2c02229
ACS Omega 2022, 7, 28118−28128

Table 2. Selected Major Reactions in the Cyclohexene Submechanism[b]

no.	reaction[a]	A	n	E_a	reference
1	$CYC_6H_{10} = C_4H_6 + C_2H_4$ (1)	5.50E + 12	0.76	62 450.00	36
2	$CYC_6H_{10} = CYHEXDN13 + H_2$ (2)	7.08E + 09	1.12	59 560.00	36
3	$CYC_6H_{10} + H = CYC_6H_9 - R1 + H_2$ (3)	5.07E + 07	1.900	12 950.00	37
4	$CYC_6H_{10} + O = CYC_6H_9 - R1 + OH$ (4)	1.51E + 07	1.90	3740.00	38
5	$CYC_6H_{10} + OH = CYC_6H_9 - R1 + H_2O$ (5)	3.60E + 06	2.00	2500.00	39
6	$CYC_6H_{10} + CH_3 = CYC_6H_9 - R1 + CH_4$ (6)	2.27E + 05	2.00	9200.00	40
7	$CYC_6H_{10} + O_2 = CYC_6H_9 - R1 + HO_2$ (7)	7.40E + 08	1.42	59 630.00	estimated from RMG[41]
8	$CYC_6H_{10} + H = CYC_6H_9 - R2 + H_2$ (8)	2.30E + 05	2.50	2490.00	analogy[16]
9	$CYC_6H_{10} + O = CYC_6H_9 - R2 + OH$ (9)	2.40E + 11	0.70	5880.00	analogy[16]
10	$CYC_6H_{10} + OH = CYC_6H_9 - R2 + H_2O$ (10)	4.14E + 06	2.00	−298.00	analogy[16]
11	$CYC_6H_{10} + CH_3 = CYC_6H_9 - R2 + CH_4$ (11)	2.94E + 00	3.50	5675.00	analogy[16]
12	$CYC_6H_{10} + O_2 = CYC_6H_9 - R2 + HO_2$ (12)	1.86E + 04	1.20	8937.00	fitted
13	$CYC_6H_{10} + H = CYC_6H_9 - R3 + H_2$ (13)	1.30E + 06	2.40	4471.00	analogy[42]
14	$CYC_6H_{10} + O = CYC_6H_9 - R3 + OH$ (14)	4.76E + 04	2.71	2106.00	analogy[42]
15	$CYC_6H_{10} + OH = CYC_6H_9 - R3 + H_2O$ (15)	2.70E + 04	2.39	393.00	analogy[42]
16	$CYC_6H_{10} + CH_3 = CYC_6H_9 - R3 + CH_4$ (16)	1.51E + 00	3.46	5480.00	analogy[42]
17	$CYC_6H_{10} + O_2 = CYC_6H_9 - R3 + HO_2$ (17)	1.48E + 08	1.42	49 080.00	estimated from RMG[41]
18	$CYC_6H_9 - R2 = CYHEXDN13 + H$ (18)	2.67E + 12	0.71	49 792.20	36
19	$CYC_6H_9 - R3 = CYHEXDN13 + H$ (19)	2.67E + 12	0.71	49 792.20	36
20	$CYC_6H_9 - R3 = CYHEXDN14 + H$ (20)	2.67E + 12	0.71	49 792.20	36

[a]Species symbols CYC_6H_{10}, CYHEXDN13, and CYHEXDN14 denote cyclohexene, cyclohexa-1,3-diene, and cyclohexa-1,4-diene, respectively. The CYC_6H_9-R1, CYC_6H_9-R2, and CYC_6H_9-R3 denote the three fuel radicals formed from abstraction reactions at the vinylic, allylic, and secondary alkyl sites, respectively. [b]Rate coefficients are in the modified Arrhenius formula as $k = AT^n \exp(-E_a/RT)$. The units are cm^3, mol, s, and K.

temperature oxidation of cyclohexane in jet-stirred reactors, and cyclohexene was detected as an important intermediate. Most recently, Giarracca et al.[21] developed a detailed kinetic mechanism to describe the combustion chemistry of four cyclo-C_6 fuels including cyclohexane, cyclohexene, 1,3-cyclohexadiene, and 1,4-cyclohexadiene to simulate the measured IDTs of the four fuels at high temperature (above 1200 K) with mean pressures of 6 atm. In addition, this work also employs the NUIGMech1.1 skeletal base model[22] to develop an updated detailed mechanism for cyclohexene oxidation kinetics at high-temperature conditions. The employed skeletal mechanism was derived from the detailed NUIGMech 1.1 mechanism, which was developed systematically and hierarchically by re-evaluating the kinetics and thermochemistry of C_0−C_4 base chemistry based on recent ab initio studies and experimental diagnostics.[23,30] The NUIGMech1.1 skeletal base model has been validated systematically for C_0−C_4 fuels and has been confirmed to be effective in the development of large fuel molecules.[22,31] Table 2 lists the major initial reactions in the cyclohexene submechanism together with the related reaction rate coefficients. Specifically, in the development of the submechanism of cyclohexene, besides these abstraction and decomposition reactions listed in Table 2, the related submechanisms of CYHEXDN13 and CYHEXDN14 are taken from the NUIGMech 1.1 mechanism,[23,30] while some lumped reactions taken from the Serinyel mechanism[29] are also added to consider the low-temperature and high-pressure effect. Besides, a submechanism for cyclopentene is implemented based on an analogy to the reaction classes of cyclohexene. Systematic analysis of the differences among the four used mechanisms is performed using sensitivity analysis and reaction path analysis. Kinetic modeling for ignition is performed using Cantera software[32] assuming a closed homogeneous batch reactor at constant volume, which has been confirmed to be adequate for kinetic simulations of shock tube IDTs from short test times (which occur at high temperatures).[33−35]

4. RESULTS AND DISCUSSION

4.1. IDT Characteristics of Cyclohexene. Figure 2 shows the measured IDTs of cyclohexene in the air with the equivalence ratios of 0.5, 1.0, and 2.0 under the pressures of 5, 10, and 20 bar and the temperature range of 945−1400 K. It is shown that for a given temperature and equivalence ratio, the pressure significantly affects the IDTs for cyclohexene. More specifically, increasing the pressure greatly reduces the IDTs. The IDTs of cyclohexene exhibit Arrhenius behaviors as a function of temperature. Generally, the IDTs of cyclohexene decrease as the equivalence ratio increases.

From Figure 2, all of the four detailed mechanisms correctly predict the variation tendencies of IDTs as a function of temperature, pressure, and equivalence ratio. However, the performance in predicting the measured absolute IDT values is still different. The JetSurF 2.0 mechanism[16] demonstrates good performance in predicting the IDTs of cyclohexene at equivalence ratios of 0.5 and 1.0, but the errors tend to become larger at an equivalence ratio of 2 and a pressure of 20 bar. The Serinyel mechanism[29] shows better performance for

https://doi.org/10.1021/acsomega.2c02229
ACS Omega 2022, 7, 28118−28128

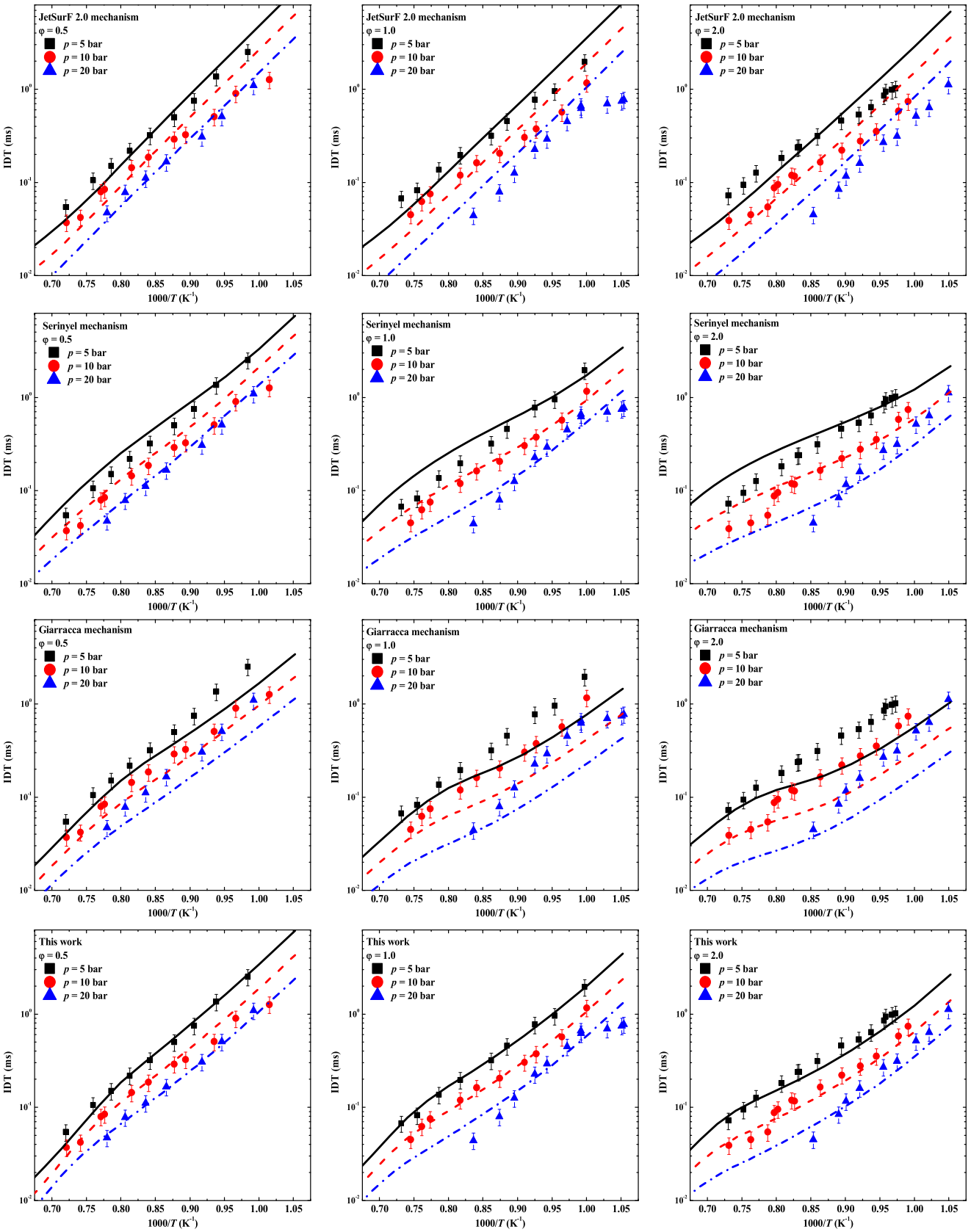

Figure 2. Comparisons of the measured and predicted IDTs for cyclohexene in this work.

most conditions except for equivalence ratios with 1.0 and 2.0 at a low-pressure condition (5 bar). The Giarracca mechanism[21] shows better performance at high-temperature conditions above 1200 K as revealed in the original aims. Finally, it can be seen that the developed mechanism in the present work exhibits good performance for all of the studied

https://doi.org/10.1021/acsomega.2c02229
ACS Omega 2022, 7, 28118−28128

combustion conditions. To show the overall different performances of the four mechanisms more specifically, statistical error analysis is carried out by calculating the standard deviation (σ), the mean absolute deviation (MAD), the mean square error (MSE), and the mean absolute percentage error (MAPE) between kinetic modeling results and experimental measurements using the following equations[43,44]

$$\mathrm{MAD} = \frac{1}{n}\sum |\mathrm{IDT}_{\mathrm{model}} - \mathrm{IDT}_{\mathrm{exp}}| \tag{21}$$

$$\sigma = \sqrt{\frac{\sum (\mathrm{IDT}_{\mathrm{model}} - \mathrm{MAD})^2}{n}} \tag{22}$$

$$\mathrm{MSE} = \frac{1}{n}\sum (\mathrm{IDT}_{\mathrm{model}} - \mathrm{IDT}_{\mathrm{exp}})^2 \tag{23}$$

$$\mathrm{MAPE} = \frac{1}{n}\sum \frac{|\mathrm{IDT}_{\mathrm{model}} - \mathrm{IDT}_{\mathrm{exp}}|}{\mathrm{IDT}_{\mathrm{exp}}} \times 100 \tag{24}$$

In the above equations, n represents the total number of measured IDTs with a value of 93. Figure 3 shows the computed error analysis values using the four kinetic modeling results. It can be seen that the comparisons shown in Figure 3 demonstrate that the present mechanism tends to perform better against the IDT measurements than the other three mechanisms.

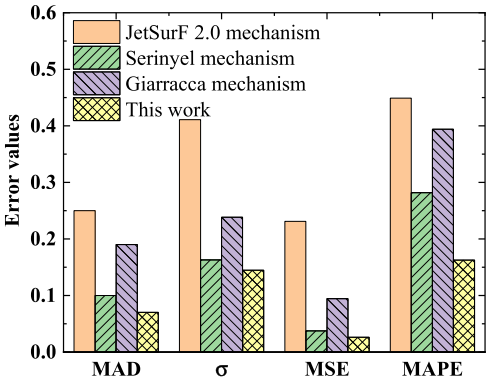

Figure 3. Statistical error analysis of the four mechanisms in the prediction of the measured IDTs of cyclohexene in this work. The MAPE values are not multiplied by 100, as shown in eq 24, for clarity.

4.2. Sensitivity Analysis Results. The detailed kinetic differences and key reactions controlling the ignition characteristics of cyclohexene are discussed in detail in the following section using sensitivity analysis and reaction path analysis. To identify key reactions affecting the ignition properties of cyclohexene, brute-force sensitivity analysis is performed using the four detailed kinetic mechanisms. Sensitivity analysis is conducted for IDT assuming a closed homogeneous batch reactor at constant volume. The sensitivity coefficient is computed via $S_i = [\tau(2{*}k_i) - \tau(k_i)]/\tau(k_i)$, in which k_i is the rate constant of reaction i, $\tau(2{*}k_i)$ is the IDT when the rate constant of reaction i is doubled, and $\tau(k_i)$ is the original predicted IDT. Thus, a negative value for sensitivity means that the ignition delay becomes shorter with increasing rate constant of reaction i, and vice versa. The sensitivity coefficients are computed through a one-by-one procedure by changing the rate constant of one reaction at a time. Sensitivity analysis is carried out using the four detailed mechanisms at 1200 K and 20 bar with equivalence ratios of 0.5, 1.0, and 2.0. Figure 4 shows the top 10 reactions that demonstrate negative and positive effects on the IDTs of cyclohexene at 1200 K and 20 bar with an equivalence ratio of 1.0, while the detailed results at equivalence ratios of 0.5 and 2.0 are provided in Supporting Materials.

From Figure 4, it is shown that the sensitive reactions in different detailed mechanisms exhibit very large differences. In the JetSurF 2.0 mechanism, the top sensitive reactions are mostly relevant to the C_0−C_4 molecules except for the initial reactions of cyclohexene (denoted as C_6H_{10}) to the formation of a 2-cyclohexenyl radical (SAXcC_6H_9) and related products and the following reactions of SAXcC_6H_9. It is worth noting that the initial abstraction reactions are simplified for cyclohexene in the JetSurF 2.0 mechanism by only considering the abstraction reactions at the allyl site to the formation of the 2-cyclohexenyl radical. At a high-pressure condition, it can be seen that the reactions of H_2O_2 show large sensitive coefficients during the oxidation of cyclohexene. Besides, the reactions relevant to 1,3-butadiene (C_4H_6) and ethylene (C_2H_4) also demonstrate a large effect on the IDT of cyclohexene since the decomposition reaction of cyclohexene to 1,3-butadiene and ethylene is the dominant reaction during the oxidation of cyclohexene as will be revealed from reaction path analysis in the following section.

In the Serinyel mechanism, a large number of the initial reactions of cyclohexene (denoted as C_6H_{10}Z#6) exhibit large sensitivity coefficients on the IDT. Unlike the JetSurF 2.0 mechanism, the two initial decomposition reactions of cyclohexene to the formation of 1,3-butadiene and ethylene (C_2H_4Z + $C_4H_6Z_2$) and 1,3-cyclohexadiene and hydrogen (C_6H_8#6-13 + H_2) show negative and positive effects on the IDT of cyclohexene, respectively, indicating that the two reactions are competitive during the oxidation of cyclohexene. In addition, besides the abstraction reactions at the allyl site to the formation of a 2-cyclohexenyl radical (denoted as $RC_2C_6H_9$#6Y), the abstraction reaction at the alkyl site by a OH radical to the formation of a 3-cyclohexenyl radical (denoted as $RC_2C_6H_9$#6Z) also plays an important role in determining the IDT, indicating the importance of considering all possible reactions to the development of a comprehensive reaction mechanism for cyclohexene combustion chemistry.

In the Giarracca mechanism, the top sensitive reactions affecting the IDT of cyclohexene tend to be much more complicated. Besides the initial decomposition and abstractions of cyclohexene (C_6H_{10}#), the reactions relevant to benzene (C_6H_6#), 2-methylcyclopentadiene (MC_2), and methylcyclopentadiene (MCPD) show a large effect on the IDT of cyclohexene, which may be probably induced by the large number of reactions relevant to the cyclic fuels involved in the research. It is also worth noting that the abstraction reactions at the vinylic site of cyclohexene are not considered in the Giarracca mechanism, which makes it not a comprehensive mechanism.

Considering the incomplete nature of the JetSurF 2.0 and Giarracca mechanisms, the present work develops a detailed mechanism for cyclohexene based on the recently derived NUIGMech1.1 skeletal mechanism with the cyclohexene submechanism initially used in the Serinyel mechanism.[19,29] Details of the updated mechanism are provided in Supporting Materials. Sensitivity analysis using the developed mechanism in the present work is very similar to the JetSurF 2.0 mechanism in that the small C_0−C_4 reactions together with the

https://doi.org/10.1021/acsomega.2c02229
ACS Omega 2022, 7, 28118−28128

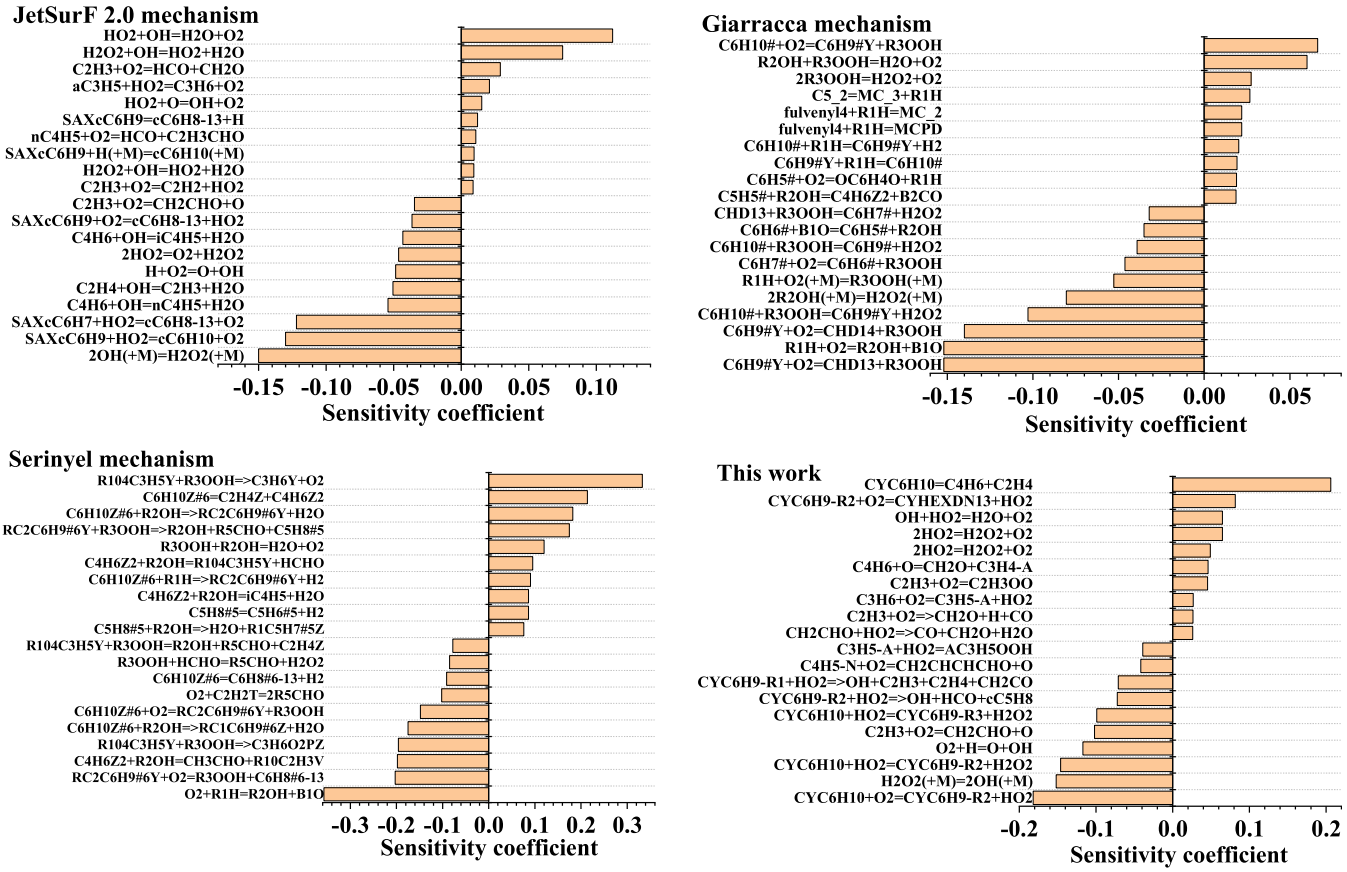

Figure 4. Brute-force sensitivity coefficient of IDT for cyclohexene at 1200 K and 20 bar with an equivalence ratio of 1.0.

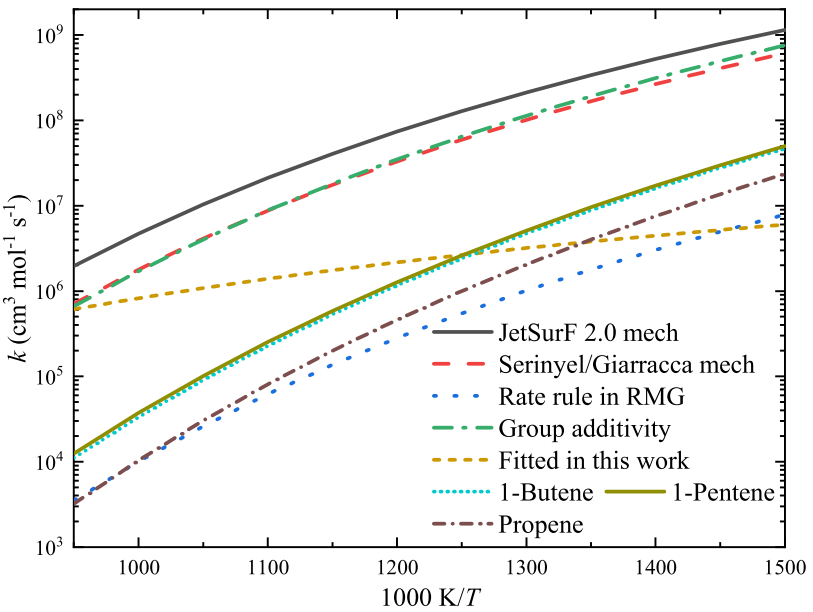

Figure 5. Rate constants as a function of temperature for the reaction cyclohexene + O_2 = 2-cyclohexenyl radical + HO_2. The lines for 1-butene and 1-pentene denote the computed reaction rate constants at the secondary allylic sites, and the line for propene represents the rate constants at the primary allylic site by Zhou et al.[45]

initial reactions of cyclohexene are the most sensitive reactions affecting the IDT of cyclohexene. However, it is also observed that the initial abstraction reaction by oxygen to the formation of the 2-cyclohexenyl radical and the HO_2 radical tends to be important in all mechanisms.

Figure 5 shows the rate constants of the abstraction reaction of cyclohexene by oxygen to the formation of the 2-cyclohexenyl radical and the HO_2 radical as a function of temperature from different mechanisms together with estimations from RMG software.[41] For comparison, the computed reaction rate constants by Zhou et al.[45] for 1-

https://doi.org/10.1021/acsomega.2c02229
ACS Omega 2022, 7, 28118−28128

butene and 1-pentene at the secondary allylic site together with those for propene at the primary allylic site were studied. The rate constants used in the JetSurF 2.0 mechanism shown in Figure 5 were fitted from the reverse reaction, which was an analogy to the rate constants of propene with oxygen.[46] The rate constants for the reverse reaction, i.e., allyl + HO_2 = C_3H_6 + O_2, are a constant value as a function of temperature, indicating that the reaction constants of propene + O_2 as a function of temperature are mainly affected via the thermodynamics properties changes. As shown in Figure 5, the computed rate constants tend to show large deviations compared with the computed results. The rate constants used in the Serinyel mechanism[19] and estimated from group additivity in RMG tend to be close because they were both based on thermochemical kinetic methods. However, the rate rules used in RMG for this reaction tend to be much lower than the other rate constants. However, the rate rules in RMG show good agreement with the computed rate constants for propene with O_2, indicating that the small molecular reaction rate constants were probably used for large reaction systems. Considering the importance of this reaction, the rate constants from this literature are initially used for kinetic modeling studies, and it is demonstrated that the rate constants of this reaction significantly affect the predicted IDTs as temperature changes. In combination with sensitivity analysis at several temperature conditions, the rate constants are refitted in the temperature range 950−1500 K, and it can be seen that the refitted rate constants lie between the literature values. Especially, at high-temperature conditions, the rate constants are very close to the rate constants for 1-butene and 1-pentene. However, at low-temperature conditions lower than 1150 K, large deviations exist among the various sources, indicating that future studies on these reaction classes are still needed because contemporary computational studies are still not accurate enough.[45] The updated mechanism in this work exhibits better performance in predicting the measured IDTs of cyclohexene at high-temperature conditions. However, further accurate estimation of the rate constants of this reaction using either a theoretical kinetic study or experimental investigation is still desired.

4.3. Reaction Path Analysis. To further demonstrate the differences in the detailed mechanisms of cyclohexene, reaction path analysis is carried out using the time-integrated element flux analysis[47−49] during the ignition simulation processes. Figure 6 shows the carbon element flux analysis results for cyclohexene during the ignition process at 1200 K and 20 bar with an equivalence ratio of 1.0 using the JetSurF 2.0, Serinyel, and present mechanisms. The results from the Giarracca mechanism are not explicitly shown due to the large deviations compared with the measured IDTs. Due to the simplicity of the submechanism in the JetSurF 2.0 mechanism, it can be seen that the reaction path for cyclohexene is rather simple. At the studied high-temperature conditions, the direct decomposition reaction of cyclohexene to ethylene and 1,3-butadiene is dominant, while the abstraction reaction at the allylic site leads to the formation of benzene. A detailed reaction path of the further oxidation of ethylene and 1,3-butadiene can be found elsewhere.[50]

The reaction path for cyclohexene oxidation from the Serinyel and present mechanisms is different compared with the JetSurF 2.0 mechanism. The completeness of the two mechanisms results in a much-complicated reaction path during the ignition of cyclohexene. The abstraction reactions

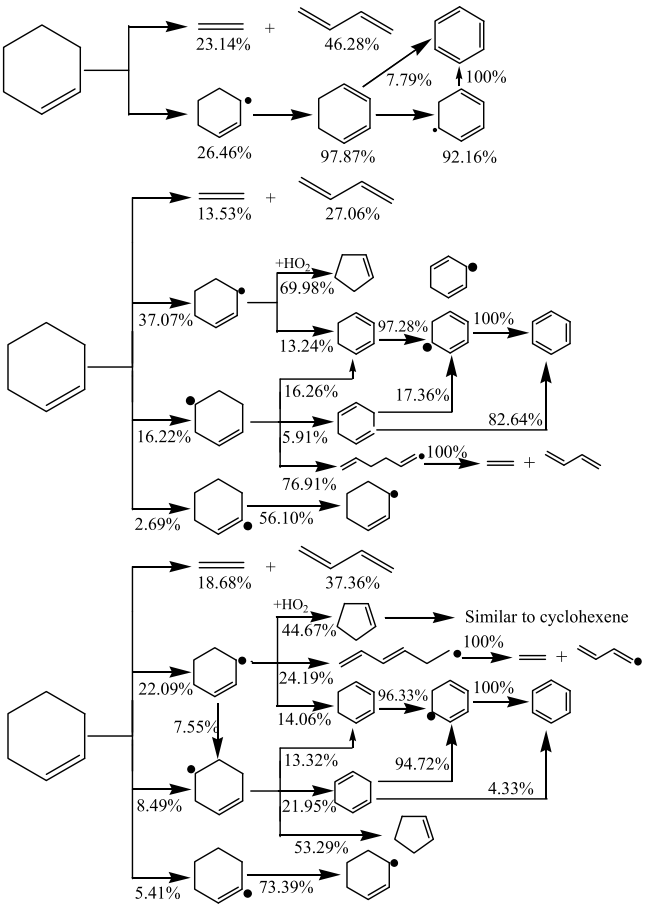

Figure 6. Percentage of the conversion calculated from the four detailed mechanisms during constant volume ignition simulation processes at 1200 K and 20 bar with an equivalence ratio of 1.0. The three reaction path analysis results from top to bottom are derived using the JetSurF 2.0, Serinyel, and present mechanisms, respectively.

can be competed with the direct decomposition reaction of cyclohexene, even though the decomposition reaction contributes higher than the other reactions. In the Serinyel mechanism, the decomposition reaction to the formation of ethylene and 1,3-butadiene consumes approximately 40% of cyclohexene, while the abstraction reactions at the three different reaction sites consumes about 60% of cyclohexene. It can be seen that the abstraction reactions to the formation of the 2-cyclohexenyl radical are dominant, which mostly converts into cyclopentene. The major reaction path derived from the present mechanism is very similar to that from the Serinyel mechanism. However, the absolute percent of conversions are different mainly due to the adopted different reaction rate constants for dominant reactions. Both the Serinyel and present mechanisms indicate that the cyclopentene submechanism should be important for cyclohexene. However, due to the lack of systematic and consistent rate constants mainly for the initial abstraction reactions of cyclopentene and cyclohexene, the accurate development of detailed kinetic mechanisms for cyclopentene and cyclohexene is still a challenge. However, the present work provides Supporting Material for further mechanism optimization.

4.4. Extended Validation of the Updated Mechanism. To further validate the present detailed mechanism, additional kinetic simulations for ignition of cyclohexene are carried out, as shown in Figure 6. It can be seen that the present detailed

https://doi.org/10.1021/acsomega.2c02229
ACS Omega 2022, 7, 28118−28128

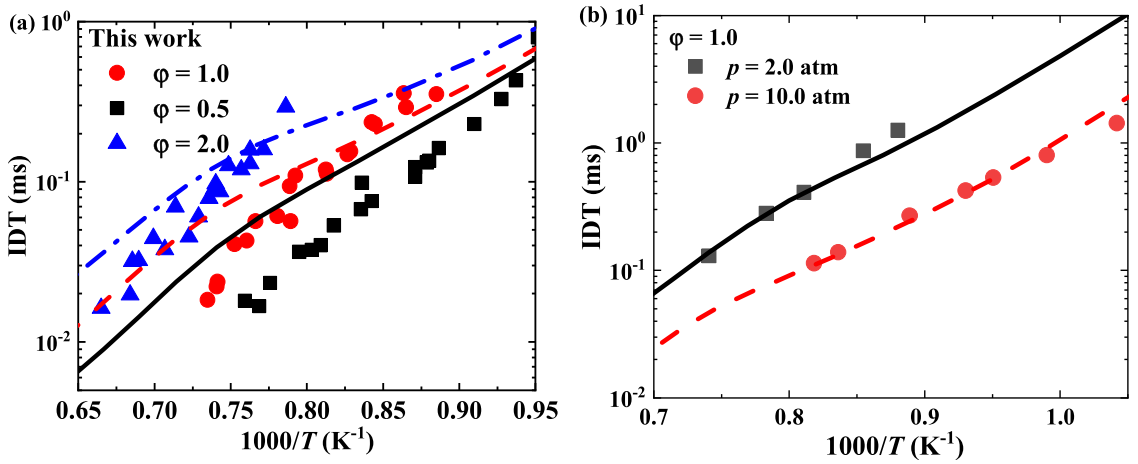

Figure 7. Extended validations of the present mechanism for IDTs of cyclohexene: (a) IDTs measured by Dayma et al.[19] (Copyright 2003 Wiley) with the averaged pressure of 8.5 bar and (b) IDTs measured by Lu et al.[51] (Copyright 2021 RSC).

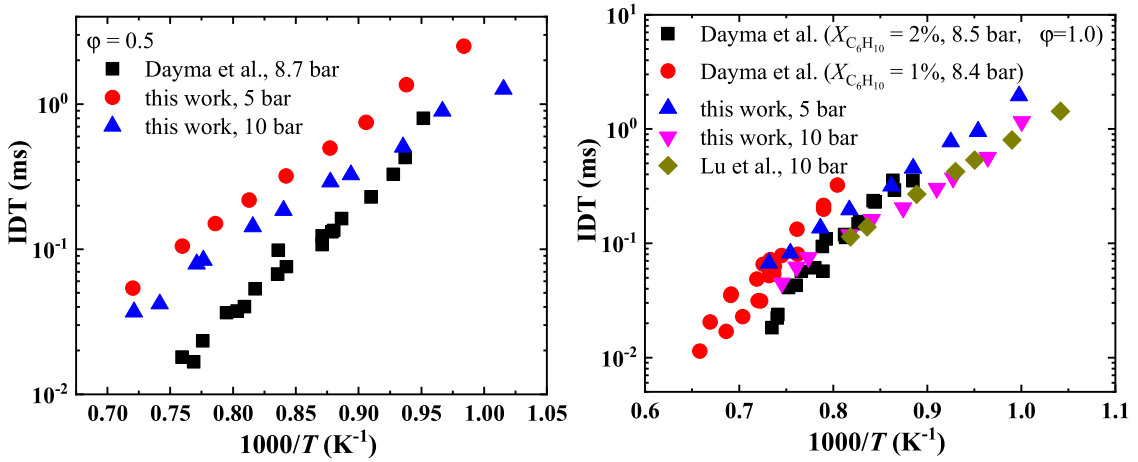

Figure 8. Comparisons of the measured IDTs for cyclohexene at different typical conditions with the results measured by Dayma et al.[19] (Copyright 2003 Wiley) and Lu et al.[51] (Copyright 2021 RSC).

mechanism also shows acceptable performance for the measured IDTs by Dayma et al.,[19] while the results for the experimental results by Lu et al.[51] are very good. Major deviations between the simulation results and experimental results are mainly induced by the measured experimental results from different groups, as shown in Figure 7. At an equivalence ratio of 0.5, it is shown that the measured IDTs at 8.7 bar tend to be faster than the present work even at 10 bar. Some of the deviations are mostly probably induced by the different diluent gases and the corresponding concentrations. From both Figures 7 and 8, it can be seen that our present experimental results are in good consistence with the results by Lu et al.[51] The different concentrations of cyclohexane, as shown by Dayma et al.,[19] also exhibit a large effect on the measured IDTs. The deviations among the measured IDTs from the three experiments are mainly distributed at high-temperature conditions above 1250 K. Overall, the present work provides an additional experimental IDT result at high-pressure conditions for kinetic model optimization.

5. CONCLUSIONS

This work reports an experimental and kinetic modeling study of the high-temperature ignition of cyclohexene under a wide range of combustion conditions. Specifically, ignition delay times (IDTs) for cyclohexene are measured in a high-pressure shock tube (HPST) with pressures of 5, 10, and 20 bar, equivalence ratios of 0.5, 1.0, and 2.0 in temperatures ranging from 980 to 1400 K. The experimental results are simulated using three previous detailed kinetic mechanisms and an updated detailed mechanism in this work. Reaction path analysis and sensitivity analysis are performed to provide insight into the chemical kinetics controlling the ignition of cyclohexene. Major conclusions are summarized as follows:

(1) The ignition characteristics of cyclohexene as a function of pressure, temperature, and equivalence ratio are systematically studied. Generally, the pressure significantly affects the IDTs for cyclohexane, and increasing the pressure greatly reduces the IDTs. The IDTs of cyclohexene exhibit Arrhenius behaviors as a function of temperature. The IDTs of cyclohexene decrease as the equivalence ratio increases. No obvious negative temperature coefficient region is observed even at a pressure up to 20 bar.

(2) Three literature detailed kinetic models are used to simulate the present experimental results, and large deviations still exist. An updated detailed kinetic model is also developed and demonstrates good agreements with the measured IDTs.

https://doi.org/10.1021/acsomega.2c02229
ACS Omega 2022, 7, 28118−28128

(3) Sensitivity analysis results indicate that the top reactions affecting the IDTs are different using different detailed mechanisms. However, it is worth noting that the most detailed mechanisms indicate that the abstraction reaction by oxygen at the allylic site is significant, even though it is not a major contribution to the consumption of cyclohexene.
(4) Reaction path analysis results reveal that different detailed kinetic mechanisms are significantly different, and until now, there are still no unified conclusions about the major reaction path for cyclohexene oxidation. It is shown that the submechanism of cyclopentene is important during the oxidation of cyclohexene.
(5) Sensitivity analysis and reaction path analysis results indicate that high-level theoretical studies in combination with experimental studies on the initial decomposition and abstraction reactions of cyclohexene and cyclopentene are imperative to develop and optimize the detailed kinetic mechanism of cyclohexene.

■ ASSOCIATED CONTENT

Supporting Information

The Supporting Information is available free of charge at https://pubs.acs.org/doi/10.1021/acsomega.2c02229.

Measured ignition delay times and sensitivity analysis results and detailed kinetic mechanism in the Cantera and Chemkin format (PDF)
Cyclohexene_mech (TXT)
Cyclohexene-therm (TXT)

■ AUTHOR INFORMATION

Corresponding Authors

Jinhu Liang − *School of Environmental and Safety Engineering, North University of China, Taiyuan 030051, People's Republic of China;* orcid.org/0000-0003-3972-7664; Email: jhliang@nuc.edu.cn

Quan-De Wang − *Jiangsu Key Laboratory of Coal-Based Greenhouse Gas Control and Utilization, Carbon Neutrality Institute and School of Chemical Engineering, China University of Mining and Technology, Xuzhou 221008, People's Republic of China;* orcid.org/0000-0002-3941-0192; Email: quandewang@cumt.edu.cn

Authors

Fei Li − *School of Environmental and Safety Engineering, North University of China, Taiyuan 030051, People's Republic of China*

Shutong Cao − *School of Environmental and Safety Engineering, North University of China, Taiyuan 030051, People's Republic of China*

Xiaoliang Li − *School of Environmental and Safety Engineering, North University of China, Taiyuan 030051, People's Republic of China*

Ruining He − *School of Environmental and Safety Engineering, North University of China, Taiyuan 030051, People's Republic of China*

Ming-Xu Jia − *Jiangsu Key Laboratory of Coal-Based Greenhouse Gas Control and Utilization, Carbon Neutrality Institute and School of Chemical Engineering, China University of Mining and Technology, Xuzhou 221008, People's Republic of China*

Complete contact information is available at: https://pubs.acs.org/10.1021/acsomega.2c02229

Notes

The authors declare no competing financial interest.

■ ACKNOWLEDGMENTS

J.L. acknowledges funding from the Natural Science Foundation of China (12172335), the International Scientific Cooperation Projects of Key R&D Programs in Shanxi Province (No. 201803D421101), and the Research Project Supported by Shanxi Scholarship Council of China (No. 2020-115); F.L. acknowledges funding from the Graduate Innovation Project of Shanxi Province (2021Y654); and Q.-D.W. acknowledges financial support from the National Natural Science Foundation of China (No. U2133215) and Fundamental Research Funds for the Central Universities of China (No. 2020ZDPYMS05).

■ REFERENCES

(1) Sarathy, S. M.; Farooq, A.; Kalghatgi, G. T. Recent progress in gasoline surrogate fuels. *Prog. Energy Combust. Sci.* **2018**, *65*, 67−108.
(2) Battin-Leclerc, F. Detailed chemical kinetic models for the low-temperature combustion of hydrocarbons with application to gasoline and diesel fuel surrogates. *Prog. Energy Combust. Sci.* **2008**, *34*, 440−498.
(3) Yang, Z.-Y.; Zeng, P.; Wang, B.-Y.; Jia, W.; Xia, Z.-X.; Liang, J.; Wang, Q.-D. Ignition characteristics of an alternative kerosene from direct coal liquefaction and its blends with conventional RP-3 jet fuel. *Fuel* **2021**, *291*, No. 120258.
(4) Westbrook, C. K.; Curran, H. J. Detailed Kinetics of Fossil and Renewable Fuel Combustion. In *Computer Aided Chemical Engineering*; Elsevier, 2019; pp 363−443.
(5) Curran, H. J. Developing detailed chemical kinetic mechanisms for fuel combustion. *Proc. Combust. Inst.* **2019**, *37*, 57−81.
(6) Das, D. D.; John, P. C. S.; McEnally, C. S.; Kim, S.; Pfefferle, L. D. Measuring and predicting sooting tendencies of oxygenates, alkanes, alkenes, cycloalkanes, and aromatics on a unified scale. *Combust. Flame* **2018**, *190*, 349−364.
(7) Pitz, W. J.; Naik, C. V.; Mhaolduin, T. N.; Westbrook, C. K.; Curran, H. J.; Orme, J. P.; Simmie, J. M. Modeling and experimental investigation of methylcyclohexane ignition in a rapid compression machine. *Proc. Combust. Inst.* **2007**, *31*, 267−275.
(8) Mittal, G.; Sung, C. J. Autoignition of methylcyclohexane at elevated pressures. *Combust. Flame* **2009**, *156*, 1852−1855.
(9) Hong, Z. K.; Lam, K. Y.; Davidson, D. F.; Hanson, R. K. A comparative study of the oxidation characteristics of cyclohexane, methylcyclohexane, and n-butylcyclohexane at high temperatures. *Combust. Flame* **2011**, *158*, 1456−1468.
(10) Wang, Z. D.; Ye, L. L.; Yuan, W. H.; Zhang, L. D.; Wang, Y. Z.; Cheng, Z. J.; Zhang, F.; Qi, F. Experimental and kinetic modeling study on methylcyclohexane pyrolysis and combustion. *Combust. Flame* **2014**, *161*, 84−100.
(11) Alekseev, V. A.; Matveev, S. S.; Chechet, I. V.; Matveev, S. G.; Konnov, A. A. Laminar burning velocities of methylcyclohexane plus air flames at room and elevated temperatures: A comparative study. *Combust. Flame* **2018**, *196*, 99−107.
(12) Bissoonauth, T.; Wang, Z. D.; Mohamed, S. Y.; Wang, J. Y.; Chen, B. J.; Rodriguez, A.; Frottier, O.; Zhang, X. Y.; Zhang, Y.; Cao, C. C.; Yang, J. Z.; Herbinet, O.; Battin-Leclerc, F.; Sarathy, S. M. Methylcyclohexane pyrolysis and oxidation in a jet-stirred reactor. *Proc. Combust. Inst.* **2019**, *37*, 409−417.
(13) Kim, S.; Fioroni, G. M.; Park, J.-W.; Robichaud, D. J.; Das, D. D.; John, P. C. S.; Lu, T.; McEnally, C. S.; Pfefferle, L. D.; Paton, R. S.; Foust, T. D.; McCormick, R. L. Experimental and theoretical insight into the soot tendencies of the methylcyclohexene isomers. *Proc. Combust. Inst.* **2019**, *37*, 1083−1090.

(14) Narayanaswamy, K.; Pitsch, H.; Pepiot, P. A chemical mechanism for low to high temperature oxidation of methylcyclohexane as a component of transportation fuel surrogates. *Combust. Flame* **2015**, *162*, 1193−1213.
(15) Ji, C. S.; Dames, E.; Sirjean, B.; Wang, H.; Egolfopoulos, F. N. An experimental and modeling study of the propagation of cyclohexane and mono-alkylated cyclohexane flames. *Proc. Combust. Inst.* **2011**, *33*, 971−978.
(16) Wang, H.; Dames, E.; Sirjean, B.; Sheen, D. A.; Tangko, R.; Violi, A.; Lai, J. Y. W.; Egolfopoulos, F. N.; Davidson, D. F.; Hanson, R. K.; Bowman, C. T.; Law, C. K.; Tsang, W.; Cernansky, N. P.; Miller, D. L.; Lindstedt, R. P. JetSurF II: a high temperature chemical kinetic model of n-alkane (up to n-dodecane), cyclohexane, and methyl-, ethyl-, n-propyl and n-butyl-cyclohexane oxidation at high temperatures, http://web.stanford.edu/group/haiwanglab/JetSurF/JetSurF2.0/.
(17) Wang, Z.; Zhao, L.; Wang, Y.; Bian, H.; Zhang, L.; Zhang, F.; Li, Y.; Sarathy, S. M.; Qi, F. Kinetics of ethylcyclohexane pyrolysis and oxidation: An experimental and detailed kinetic modeling study. *Combust. Flame* **2015**, *162*, 2873−2892.
(18) Zou, J.; Zhang, X.; Li, Y.; Ye, L.; Xing, L.; Li, W.; Cao, C.; Zhai, Y.; Qi, F.; Yang, J. Experimental and kinetic modeling investigation on ethylcyclohexane low-temperature oxidation in a jet-stirred reactor. *Combust. Flame* **2020**, *214*, 211−223.
(19) Dayma, G.; Glaude, P. A.; Fournet, R.; Battin-Leclerc, F. Experimental and modeling study of the oxidation of cyclohexene. *Int. J. Chem. Kinet.* **2003**, *35*, 273−285.
(20) Wang, J.; Sun, W.; Wang, G.; Fan, X.; Lee, Y.-Y.; Law, C. K.; Qi, F.; Yang, B. Understanding benzene formation pathways in pyrolysis of two C6H10 isomers: Cyclohexene and 1,5-hexadiene. *Proc. Combust. Inst.* **2019**, *37*, 1091−1098.
(21) Giarracca, L.; Isufaj, F.; Lizardo-Huerta, J. C.; Fournet, R.; Glaude, P. A.; Sirjean, B. Experimental and kinetic modeling of the ignition delays of cyclohexane, cyclohexene, and cyclohexadienes: Effect of unsaturation. *Proc. Combust. Inst.* **2021**, *38*, 1017−1024.
(22) Wang, Q.-D.; Panigrahy, S.; Yang, S.; Martinez, S.; Liang, J.; Curran, H. J. Development of Multipurpose Skeletal Core Combustion Chemical Kinetic Mechanisms. *Energy Fuels* **2021**, *35*, 6921−6927.
(23) Panigrahy, S.; Liang, J.; Ghosh, M. K.; Wang, Q.-D.; Zuo, Z.; Nagaraja, S.; Mohamed, A. A. E.-S.; Kim, G.; Vasu, S. S.; Curran, H. J. An experimental and detailed kinetic modeling study of the pyrolysis and oxidation of allene and propyne over a wide range of conditions. *Combust. Flame* **2021**, *233*, No. 111578.
(24) Morley, C. *Gaseq: A Chemical Equilibrium Program for Windows, 0.79*, 2005.
(25) Panigrahy, S.; Liang, J.; Nagaraja, S. S.; Zuo, Z.; Kim, G.; Dong, S.; Kukkadapu, G.; Pitz, W. J.; Vasu, S. S.; Curran, H. J. A comprehensive experimental and improved kinetic modeling study on the pyrolysis and oxidation of propyne. *Proc. Combust. Inst.* **2021**, *38*, 479−488.
(26) Baigmohammadi, M.; Patel, V.; Nagaraja, S.; Ramalingam, A.; Martinez, S.; Panigrahy, S.; Mohamed, A. A. E.-S.; Somers, K. P.; Burke, U.; Heufer, K. A.; Pekalski, A.; Curran, H. J. Comprehensive Experimental and Simulation Study of the Ignition Delay Time Characteristics of Binary Blended Methane, Ethane, and Ethylene over a Wide Range of Temperature, Pressure, Equivalence Ratio, and Dilution. *Energy Fuels* **2020**, *34*, 8808−8823.
(27) Guzman, J.; Kukkadapu, G.; Brezinsky, K.; Westbrook, C. Experimental and modeling study of the pyrolysis and oxidation of an iso-paraffinic alcohol-to-jet fuel. *Combust. Flame* **2019**, *201*, 57−64.
(28) Mulvihill, C. R.; Mathieu, O.; Petersen, E. L. H_2O time histories in the H_2-NO_2 system for validation of NOx hydrocarbon kinetics mechanisms. *Int. J. Chem. Kinet.* **2019**, *51*, 669−678.
(29) Serinyel, Z.; Herbinet, O.; Frottier, O.; Dirrenberger, P.; Warth, V.; Glaude, P. A.; Battin-Leclerc, F. An experimental and modeling study of the low- and high-temperature oxidation of cyclohexane. *Combust. Flame* **2013**, *160*, 2319−2332.
(30) Ramalingam, A.; Panigrahy, S.; Fenard, Y.; Curran, H.; Heufer, K. A. A chemical kinetic perspective on the low-temperature oxidation of propane/propene mixtures through experiments and kinetic analyses. *Combust. Flame* **2021**, *223*, 361−375.
(31) Li, S.; Lu, H.; Mao, Y.; Zhang, C.; Huang, S.; Jiang, R.; Zhu, Q.; Yang, H. Experimental and kinetic modeling study on ignition characteristic of 0# diesel in a shock tube. *Combust. Flame* **2022**, *242*, No. 112171.
(32) Goodwin, D. G.; Speth, R. L.; Moffat, H. K.; Weber, B. W. *An Object-Oriented Software Toolkit for Chemical Kinetics, Thermodynamics, and Transport Processes*, version 2.4.0, 2018.
(33) Davidson, D. F.; Hanson, R. K. Recent advances in shock tube/laser diagnostic methods for improved chemical kinetics measurements. *Shock Waves* **2009**, *19*, 271−283.
(34) Pang, G. A.; Davidson, D. F.; Hanson, R. K. Experimental study and modeling of shock tube ignition delay times for hydrogen-oxygen-argon mixtures at low temperatures. *Proc. Combust. Inst.* **2009**, *32*, 181−188.
(35) Sung, C. J.; Curran, H. J. Using rapid compression machines for chemical kinetics studies. *Prog. Energy Combust. Sci.* **2014**, *44*, 1−18.
(36) Sirjean, B.; Glaude, P. A.; Ruiz-Lopez, M. F.; Fournet, R. Theoretical Kinetic Study of the Reactions of Cycloalkylperoxy Radicals. *J. Phys. Chem. A* **2009**, *113*, 6924−6935.
(37) Knyazev, V. D.; Bencsura, Á.; Stoliarov, S. I.; Slagle, I. R. Kinetics of the C2H3 + H2 ⇄ H + C2H4 and CH3 + H2 ⇄ H + CH4 Reactions. *J. Phys. Chem. A* **1996**, *100*, 11346−11354.
(38) Mahmud, K.; Marshall, P.; Fontijn, A. A high-temperature photochemistry kinetics study of the reaction of oxygen(3P) atoms with ethylene from 290 to 1510 K. *J. Phys. Chem. B* **1987**, *91*, 1568−1573.
(39) Liu, A.; Mulac, W. A.; Jonah, C. D. Rate constants for the gas-phase reactions of hydroxyl radicals with 1,3-butadiene and allene at 1 atm in argon and over the temperature range 305-1173 K. *J. Phys. Chem. C* **1988**, *92*, 131−134.
(40) Smith, G. P.; Golden, D. M.; Frenklach, M.; Moriarty, N. W.; Eiteneer, B.; Goldenberg, M.; Bowman, C. T.; Hanson, R. K.; Song, S.; Gardiner, W. C., Jr GRI 3.0 Mechanism, 1999. http://combustion.berkeley.edu/gri-mech/releases.html.
(41) Liu, M.; Dana, A. G.; Johnson, M. S.; Goldman, M. J.; Jocher, A.; Payne, A. M.; Grambow, C. A.; Han, K.; Yee, N. W.; Mazeau, E. J.; Blondal, K.; West, R. H.; Goldsmith, C. F.; Green, W. H. Reaction Mechanism Generator v3.0: Advances in Automatic Mechanism Generation. *J. Chem. Inf. Model.* **2021**, *61*, 2686−2696.
(42) Tsang, W. Chemical Kinetic Data Base for Combustion Chemistry. Part 3: Propane. *J. Phys. Chem. Ref. Data* **1988**, *17*, 887−951.
(43) Martinez, S.; Baigmohammadi, M.; Patel, V.; Panigrahy, S.; Sahu, A. B.; Nagaraja, S. S.; Ramalingam, A.; Mohamed, A. A. S.; Somers, K. P.; Heufer, K. A.; Pekalski, A.; Curran, H. J. An experimental and kinetic modeling study of the ignition delay characteristics of binary blends of ethane/propane and ethylene/propane in multiple shock tubes and rapid compression machines over a wide range of temperature, pressure, equivalence ratio, and dilution. *Combust. Flame* **2021**, *228*, 401−414.
(44) Sahu, A. B.; Mohamed, A. A. E.-S.; Panigrahy, S.; Saggese, C.; Patel, V.; Bourque, G.; Pitz, W. J.; Curran, H. J. An experimental and kinetic modeling study of NOx sensitization on methane autoignition and oxidation. *Combust. Flame* **2022**, *238*, No. 111746.
(45) Zhou, C. W.; Simmie, J. M.; Somers, K. P.; Goldsmith, C. F.; Curran, H. J. Chemical Kinetics of Hydrogen Atom Abstraction from Allylic Sites by $^3O_2$; Implications for Combustion Modeling and Simulation. *J. Phys. Chem. A* **2017**, *121*, 1890−1899.
(46) Baulch, D. L.; Cobos, C. J.; Cox, R. A.; Esser, C.; Frank, P.; Just, T.; Kerr, J. A.; Pilling, M. J.; Troe, J.; Walker, R. W.; Warnatz, J. Evaluated Kinetic Data for Combustion Modelling. *J. Phys. Chem. Ref. Data* **1992**, *21*, 411−734.
(47) Wang, Q.-D.; Fang, Y.-M.; Wang, F.; Li, X.-Y. Systematic analysis and reduction of combustion mechanisms for ignition of

https://doi.org/10.1021/acsomega.2c02229
ACS Omega 2022, 7, 28118−28128

multi-component kerosene surrogate. *Proc. Combust. Inst.* **2013**, *34*, 187−195.
(48) Zhang, S.; Broadbelt, L. J.; Androulakis, I. P.; Ierapetritou, M. G. Comparison of Biodiesel Performance Based on HCCI Engine Simulation Using Detailed Mechanism with On-the-fly Reduction. *Energy Fuels* **2012**, *26*, 976−983.
(49) He, K.; Ierapetritou, M. G.; Androulakis, I. P. Exploring flux representations of complex kinetics networks. *AlChE J.* **2012**, *58*, 553−567.
(50) Wang, Q.-D. Skeletal Mechanism Generation for High-Temperature Combustion of H_2/CO/C_1-C_4 Hydrocarbons. *Energy Fuels* **2013**, *27*, 4021−4030.
(51) Lu, H.; Kong, W.; Zhang, C.; Wang, J.; Li, X. The kinetic model of cyclohexene−air combustion over a wide temperature range. *RSC Adv.* **2021**, *11*, 39907−39916.

https://doi.org/10.1021/acsomega.2c02229
ACS Omega 2022, 7, 28118−28128